

Full Paper

Synthesis and Biological Evaluation of Some *N*-Arylpyrazoles and Pyrazolo[3,4-*d*]pyridazines as Anti-Inflammatory Agents

Osama I. El-Sabbagh^{1,2}, Samia Mostafa³, Hatem A. Abdel-Aziz^{4,5}, Hany S. Ibrahim⁶, and Mahmoud M. Elasser⁷

¹ Faculty of Pharmacy, Pharmaceutical Chemistry Department, Taif University, Taif, Saudi Arabia

² Faculty of Pharmacy, Medicinal Chemistry Department, Zagazig University, Zagazig, Egypt

³ Faculty of Pharmacy, Pharmaceutical Chemistry Department, Suez Canal University, Ismailia, Egypt

⁴ Department of Pharmaceutical Chemistry, College of Pharmacy, King Saud University, Riyadh, Saudi Arabia

⁵ Applied Organic Chemistry Department, National Research Center, Dokki, Cairo, Egypt

⁶ Faculty of Pharmacy, Department of Pharmaceutical Chemistry, Egyptian Russian University, Badr City, Helwan, Egypt

⁷ The Regional Center for Mycology and Biotechnology, Al-Azhar University, Cairo, Egypt

A series of 3,4-bis-chalcone-*N*-arylpyrazoles **3a–k** was prepared from diacetyl pyrazoles **2a–e**. The reaction of **2d** and **2e** with hydrazine hydrate gave pyrazolo[3,4-*d*]pyridazine derivatives **4a–b**. Furthermore, the reaction of **2a–e** with thiosemicarbazide afforded pyrazolo[3,4-*d*]pyridazine thiocyanate salts **5a–e**. The synthesized compounds were subjected to *in vivo* anti-inflammatory and ulcerogenic activity measurements, in addition to determination of their *in vitro* COX selectivity, to give a full profile about their anti-inflammatory activities. Compounds **3c**, **3f**, **3i**, and **3e** showed significant anti-inflammatory activity among the synthesized compounds. Moreover, docking studies were performed to give an explanation for their anti-inflammatory activity through COX selectivity.

Keywords: Anti-inflammatory activity / COX selectivity / Molecular docking / *N*-Aryl pyrazoles / Pyrazolopyridazine

Received: May 24, 2013; Revised: July 14, 2013; Accepted: July 16, 2013

DOI 10.1002/ardp.201300193

Introduction

Prostaglandins are important biological mediators of inflammation, originating from the biotransformation of arachidonic acid catalyzed by cyclooxygenases [1]. The discovery that cyclooxygenase enzyme in arachidonic acid metabolism exists in two isoforms, namely, COX-1 and COX-2 (the constitutive and inducible forms), has generated new avenues for drug design.

It was proposed that a selective inhibitor of COX-2 would be an attractive approach for the treatment of inflammatory conditions without concomitant gastric and renal toxicity [2]. Celecoxib and other coxibs, such as rofecoxib [3], etoricoxib [4], and valdecoxib [5], are selective COX-2 inhibitors with fewer gastrointestinal side effects than traditional NSAIDs.

N-Arylpyrazoles were found to be a main pharmacophore in these selective anti-inflammatory agents as celecoxib [6] and SC-558 [7, 8] (Fig. 1).

Certain chalcone derivatives were reported to possess analgesic and antipyretic actions [9, 10] in addition to their marked anti-inflammatory activity [11–14]. Among the chalcones [15, 16], 2,4-dichloro-4'-*N*-[*N'*-(4''-methylphenylsulfenyl)urenyl]chalcone (Me-UCH9) was found to exert anti-inflammatory action [15] through dual inhibition of cyclooxygenase-2 and 5-lipoxygenase activities (Fig. 1).

This motivated us to design and synthesize new series of bis-chalcones derivatives containing the *N*-aryl pyrazole moiety, which fulfill the pattern of COX-2 inhibition in order to produce potent anti-inflammatory agents with no or less gastric ulceration. In addition, the relation between the variations of substituents on the biological activity will be studied as well as molecular docking studies will be done after *in vitro* studies to analyze their mechanism of action as anti-inflammatory agents.

Correspondence: Prof. Osama I. El-Sabbagh, Pharmaceutical Chemistry Department, College of Pharmacy, Taif University, P.O. Box 888, 21974 Al-Haweiah, Taif, Saudi Arabia.

E-mail: osamaelsabbagh@yahoo.com

Fax: +966-02-7274299

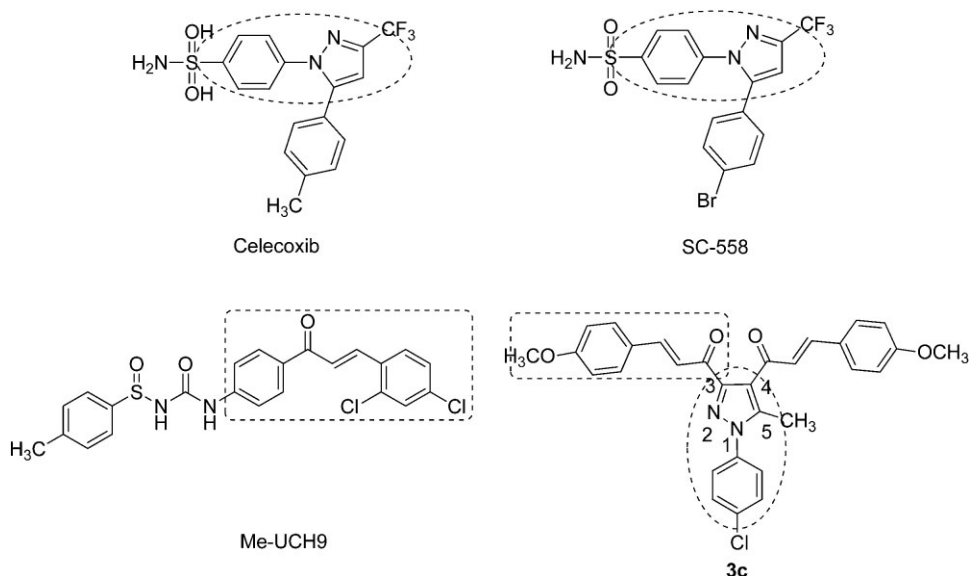


Figure 1. Chemical structures of celecoxib, SC-558, Me-UCH9, and compound **3c**.

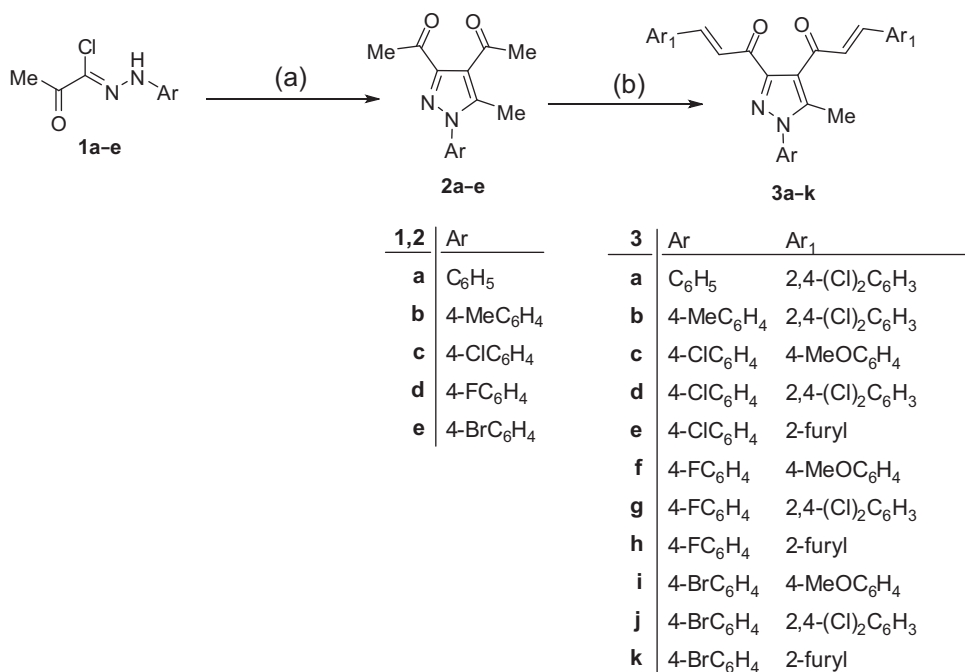
Results and discussion

Chemistry

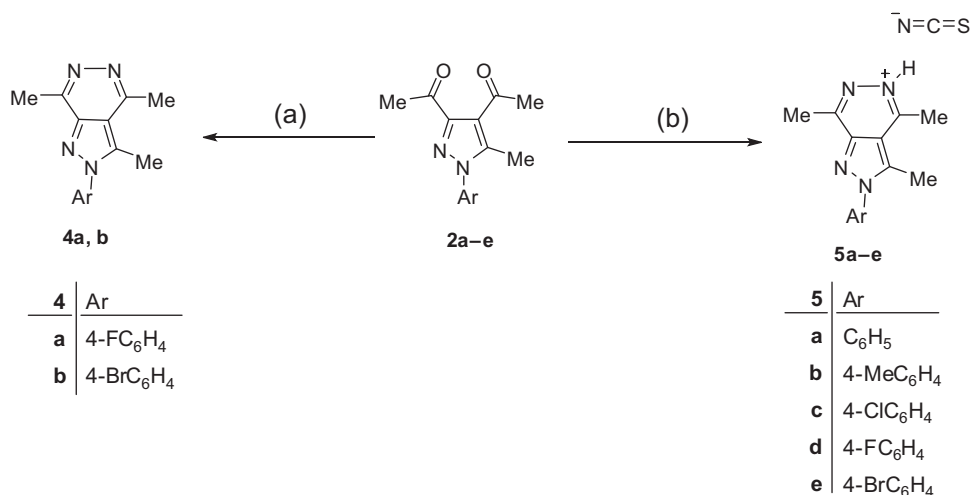
The reaction of 2-oxo-*N'*-arylpropanehydrazonoyl chlorides **1a–e** with pentan-2,4-dione in ethanol containing sodium

ethoxide gave 3,4-diacetyl-5-methyl-*N*-arylpyrazoles **2a–e** [14, 17], as shown in Scheme 1.

The reaction of the latter pyrazoles, at room temperature, with different aldehydes in the presence of aqueous sodium hydroxide afforded the bis-chalcone derivatives **3a–k**. The



Scheme 1. Synthetic pathway of compounds **2a–e** and **3a–k**. Reagents and conditions: (a) (CH₃CO)₂CH₂, EtONa/EtOH, RT, stirring 8 h; (b) 2Ar₁-CHO, EtOH, 10% NaOH, RT, stirring 6 h.



Scheme 2. Synthetic pathway of compounds **4a–b** and **5a–e**. Reagents and conditions: (a) $\text{NH}_2\text{NH}_2 \cdot \text{H}_2\text{O}$, EtOH, reflux 8 h; (b) $\text{NH}_2\text{NHCSNH}_2$, AcOH/ H_2O , reflux 4 h.

structures of the bis-chalcone derivatives **3a–k** were confirmed using IR and ^1H NMR whereas their IR spectra revealed the appearance of a strong absorption band at $\nu = 1655\text{--}1670\text{ cm}^{-1}$ for the two carbonyl groups, which are in lower range than that for the corresponding compounds **2a–e**. Moreover, the ^1H NMR spectra confirmed the structures of compounds **3a–k**. The two signals of the two COCH_3 groups at $\delta = 2.712$ and 2.96 ppm for the starting compounds **2a–e** disappeared while two signals of olefinic protons appeared in the aromatic region at $\delta = 6.8\text{--}8.0$ ppm.

Furthermore, the reaction of pyrazole derivatives **2d–e** with hydrazine hydrate in ethanol afforded pyrazolo[3,4-*d*]pyridazine derivatives **4a–b** (Scheme 2). The structures of the novel pyrazolo[3,4-*d*]pyridazine **4a–b** were established using IR and ^{13}C NMR whereas their IR spectra revealed the absence of absorption band at $\nu = 1720$ and 1723 cm^{-1} due to carbonyl groups for the starting diacetyl pyrazoles (**2d–e**). Moreover, ^{13}C NMR confirmed the structures of pyrazolo[3,4-*d*]pyridazines (**4a–b**) whereas the two peaks of the two COCH_3 groups, which appeared around $\delta = 27.6\text{--}31.7$ ppm for the starting **2d–e**, were shifted to the range $\delta = 18.0\text{--}20.7$ ppm.

Our attempt to synthesize bis-thiosemicarbazone derivatives of diacetyl pyrazoles **2a–e** gave the pyrazolo[3,4-*d*]pyridazine thiocyanate salts **5a–e**. The suggested mechanism of the latter cyclization is postulated in Fig. 2. Due to the higher electrophilicity of the acetyl group at position 3 of the pyrazole moiety, the cyclization process takes place initially by the formation of its thiosemicarbazone I. The nucleophilic attack of the other hydrazino nitrogen on carbonyl group at position 4 afforded the unstable hydroxyl intermediate II, which rearranged to give intermediate III. The latter non-isolable intermediate lost an H_2O molecule to give structure IV, which rearranged to afford the final isolable salts **5a–e**.

The structure of the novel pyrazolo[3,4-*d*]pyridazin-5-ium isothiocyanate derivatives was proved using IR and ^{13}C NMR whereas IR revealed the presence of the absorption band of the thiocyanate function around 2040 cm^{-1} in addition to the absence of absorption band at $\nu = 1720$ and 1723 cm^{-1} due to carbonyl groups for the starting diacetyl pyrazoles (**2a–e**). Moreover, ^{13}C NMR confirmed the structures of compounds **5a–e** whereas the two peaks of the two acetyl groups, which appeared around $27.6\text{--}31.70$ ppm for the starting diacetyl pyrazoles (**2a–e**), were shifted to the range around 18.0 ppm. The previous results were confirmed by X-ray crystallography for compound **5b** [18].

Biological evaluation

The first target of the biological activity was to examine the anti-inflammatory activity for all compounds (**2a–e**, **3a–k**, **4a–b** and **5a–e**) via carrageenan-induced edema method [19]. Moreover, compounds that possessed a marked anti-inflammatory activity in rat paw edema test were subjected to ulcerogenic activity test [20] using celecoxib and indomethacin as reference drugs. The second target was to study the mechanism of action of these compounds through inhibition of ovine COX-1 and COX-2 using an enzyme immunoassay (EIA) kit [21].

In vivo anti-inflammatory activity

The anti-inflammatory activity for all compounds was determined via rat paw edema test [19] using celecoxib and indomethacin as reference drugs. Through analysis of Table 1, it was generally noted that the diacetyl pyrazoles (**2a–e**) showed lower anti-inflammatory activity than their corresponding bis-chalcone derivatives (**3a–k**). This is clear on comparing the activity of diacetyl pyrazole (**2c**), which caused

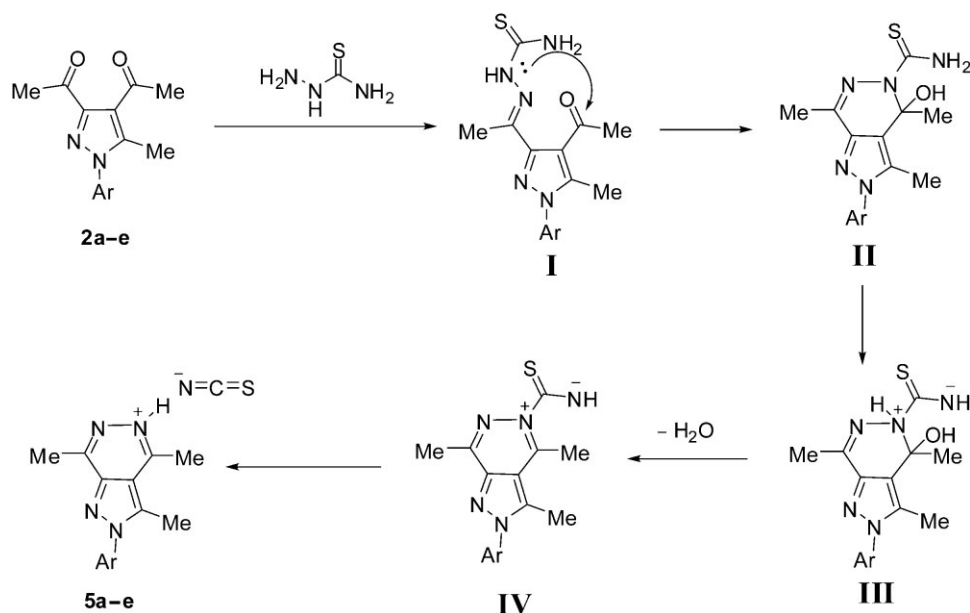


Figure 2. The proposed mechanism for the synthesis of compounds **5a–e**.

reduction of edema by 3.93%, with its corresponding bis-chalcone derivative (**3c**), which decreased the inflammation by 66.21% (Table 1).

Moreover, it was observed that the bis-chalcone derivatives **3c**, **3f**, **3i**, and **3e** showed the highest anti-inflammatory activity. The rank order of potency for such compounds is: indomethacin > **3c** > **3f** > celecoxib > **3i** > **3e**.

We observe that compounds **3c**, **3f**, and **3i** had a common *p*-methoxyphenyl as a chalcone substituent. From these results, we could deduce that chloro substituent on *N*-aryl pyrazole substituent, as seen in compound **3c**, gave the maximum activity (Table 1).

Furthermore, the bis-chalcone derivatives **3e** and **3h** bearing furyl moiety exhibited a moderate activity (Table 1). Cyclization of the diacetyl pyrazoles (**2a–e**) showed a lower or no anti-inflammatory activity as seen in the pyrazolo-pyridazine derivatives (**4a–b**, **5a–e**).

Ulcerogenic activity

Compounds **3c**, **3f**, **3i**, and **3e** that possessed the highest anti-inflammatory activity in rat paw edema test were subjected to ulcerogenic activity test [20]. Celecoxib and indomethacin were used as reference drugs. The results most likely to be withdrawn from Table 1 are:

- The order of ulcerogenic activity is: indomethacin > **3i** > **3e** > **3f** > **3c** > celecoxib.
- It was also observed that the bis-chalcone **3c** has nearly the same ulcerogenic activity as the selective COX-2 inhibitor celecoxib.

- On the other side, the chalcone **3i** exhibited a high ulcerogenic activity but it is still lesser than that of the reference drug indomethacin (Table 1).

In vitro cyclooxygenase inhibition assay

Compounds **3c**, **3f**, **3i**, and **3e** that had the highest anti-inflammatory activity in rat paw edema test were studied for their mechanism of action through inhibition of ovine COX-1 and COX-2 using an EIA kit [21].

The efficacies of the tested compounds were determined as the concentration causing 50% enzyme inhibition (IC_{50} ; Table 1). As far as COX-1 inhibitory properties are concerned, all the tested compounds showed no inhibition of COX-1 up to 100 μ M except **3e** and **3i**, as they possessed little inhibition. Moreover, a reasonable *in vitro* COX-2 inhibitory activity was observed with compounds **3c**, **3f**, **3e**, and **3i**. Selectivity index was a parameter used to diagnose the selectivity between two isoenzymes. The selectivity indices (COX-1/COX-2) were calculated and compared with those of the selective COX-2 inhibitor celecoxib.

In the assay system, the IC_{50} values of celecoxib on COX-1 and COX-2 were determined to be >100 and 0.29 μ M, indicating that celecoxib is a selective COX-2 inhibitor (SI = 344.82). The results showed that compound **3c** showed potent inhibition against COX-2 (IC_{50} = 0.30 μ M) compared to the inhibition against COX-1 (IC_{50} > 100 μ M), as listed in Table 1. Thus, compound **3c** gave the highest selectivity index (SI = 333.33). This indicates that compound **3c**, which

Table 1. Biological evaluation of the synthesized compounds.

Compounds	<i>In vivo</i> studies					<i>In vitro</i> studies			
	Size of the hind paw (mm) ^{a)}			% Edema inhibition (3 h)	% Edema inhibition (6 h)	Ulcer index ^{b)}	COX-1 IC ₅₀ (μM) ^{c)}	COX-2 IC ₅₀ (μM)	SI ^{d)}
	Before treatment with the drug	3 h after treatment	6 h after treatment						
2a	1.62 ± 0.22	4.20 ± 0.16	3.98 ± 0.16*	7.86	15.71	–	–	–	–
2b	1.78 ± 0.26	4.33 ± 0.22	4.25 ± 0.13	8.93	11.79	–	–	–	–
2c	1.29 ± 0.16	3.86 ± 0.20	3.98 ± 0.24	8.21	3.93	–	–	–	–
2d	1.88 ± 0.20	4.56 ± 0.22	4.35 ± 0.19	4.29	11.79	–	–	–	–
2e	1.90 ± 0.12	4.53 ± 0.26	4.39 ± 0.22	6.07	11.07	–	–	–	–
3a	1.66 ± 0.10	4.32 ± 0.26	4.10 ± 0.19	5.00	12.86	–	–	–	–
3b	1.55 ± 0.23	3.95 ± 0.11*	4.05 ± 0.12	14.29	10.71	–	–	–	–
3c	1.55 ± 0.16	2.80 ± 0.16***	2.50 ± 0.11***	55.29	66.21	0.90 ± 0.33 ^{b)}	>100	0.30	333.33
3d	1.23 ± 0.12	3.70 ± 0.16	3.60 ± 0.16	11.79	15.36	–	–	–	–
3e	1.88 ± 0.11	4.00 ± 0.11**	3.90 ± 0.22**	24.29	27.86	2.1 ± 0.23 ^{ab)}	78	1.5	65.333
3f	1.33 ± 0.09	2.63 ± 0.23***	2.31 ± 0.20***	53.64	65.21	1.1 ± 0.35 ^{b)}	>100	0.32	312.5
3g	1.44 ± 0.18	3.98 ± 0.18*	3.86 ± 0.12**	9.29	13.57	–	–	–	–
3h	1.80 ± 0.24	4.20 ± 0.13**	4.13 ± 0.23**	14.29	16.79	–	–	–	–
3i	1.80 ± 0.19	3.61 ± 0.18**	3.76 ± 0.22**	35.14	29.93	2.75 ± 0.25 ^{ab)}	57	0.7	76
3j	1.35 ± 0.28	4.20 ± 0.16	3.89 ± 0.18	0.00	9.29	–	–	–	–
3k	1.55 ± 0.23	4.05 ± 0.24	4.32 ± 0.16	10.71	1.07	–	–	–	–
4a	1.55 ± 0.16	4.31 ± 0.25	4.26 ± 0.23	1.43	3.21	–	–	–	–
4b	1.55 ± 0.13	4.35 ± 0.12	4.45 ± 0.13	0.00	0.00	–	–	–	–
5a	1.35 ± 0.25	3.70 ± 0.24	3.90 ± 0.18	16.07	8.93	–	–	–	–
5b	1.65 ± 0.22	3.80 ± 0.16*	3.98 ± 0.13*	23.21	16.79	–	–	–	–
5c	1.89 ± 0.23	4.20 ± 0.23	4.45 ± 0.23	17.50	8.57	–	–	–	–
5d	1.55 ± 0.13	4.23 ± 0.13	4.31 ± 0.23	4.29	1.43	–	–	–	–
5e	1.30 ± 0.12	3.78 ± 0.12	3.88 ± 0.13	11.43	7.86	–	–	–	–
Celecoxib	1.57 ± 0.14	2.95 ± 0.14***	2.56 ± 0.23***	50.71	64.64	0.83 ± 0.1 ^{b)}	>100	0.29	344.82
Indomethacin	1.45 ± 0.23	2.85 ± 0.24***	2.45 ± 0.09***	70.13	78.45	3.17 ± 0.3 ^{a)}	–	–	–
Control	1.90 ± 0.12	4.70 ± 0.19	4.90 ± 0.13	–	–	0.25 ± 0.11 ^{ab)}	–	–	–

^{a)} For rat paw edema: values represent means ± SEM of six animals for each group. Statistical analysis using one-way ANOVA (Bonferroni's multiple comparison test). Significance levels * $p < 0.5$, ** $p < 0.01$, and *** $p < 0.001$ as compared with the respective control.

^{b)} Significance level for ulcer index: ^{a)} $p < 0.05$ significantly different from celecoxib and ^{b)} $p < 0.05$ significantly different from indomethacin.

^{c)} IC₅₀ value is the compound concentration required to produce 50% inhibition of COX-1 or COX-2 for means of two determinations and deviation from the mean is <10% of the mean value. No inhibition of COX-1 up to 100 μM and precipitation of compounds was observed beyond this concentration.

^{d)} Selectivity index (COX-1 IC₅₀/COX-2 IC₅₀).

contains two *p*-methoxyphenyl groups on the chalcone wings and *p*-chloro substituent on *N*-aryl pyrazole part, gave the highest activity.

Molecular docking studies

To investigate potential binding modes of these anti-inflammatory compounds, a docking study was carried out using the most potent compound in the series (3c). Using the reported X-ray structure of COX-2 enzyme co-crystallized with SC-558 (PDB entry 1CX2) [8], an automated dock run was conducted using Molsoft ICM-pro software. Docking simulation of 3c (Fig. 3) shows that this compound gives a conformational stack energy score (–55.67 kcal/mol)

with RMSD value (1.49 Å). Compound 3c can form four hydrogen bonds within the binding pocket (Fig. 3), one of them with Arg120 (distance = 2.7 Å) by the methoxy group and second one with Arg513 (distance = 2.5 Å) by one of the carbonyl groups of the chalcone wings. The other carbonyl group can form two hydrogen bonds with Arg513 (distance = 2.49 Å) and Hip90 (distance = 2.49 Å).

One of the *p*-methoxyphenyl chalcone wings showed an interesting interaction within the binding site (Fig. 4). Actually, it was embedded inside two essential amino acids for the activity in the binding site, which are Arg120 and Tyr 335. In addition, methoxy group could form hydrogen bond with the most important amino

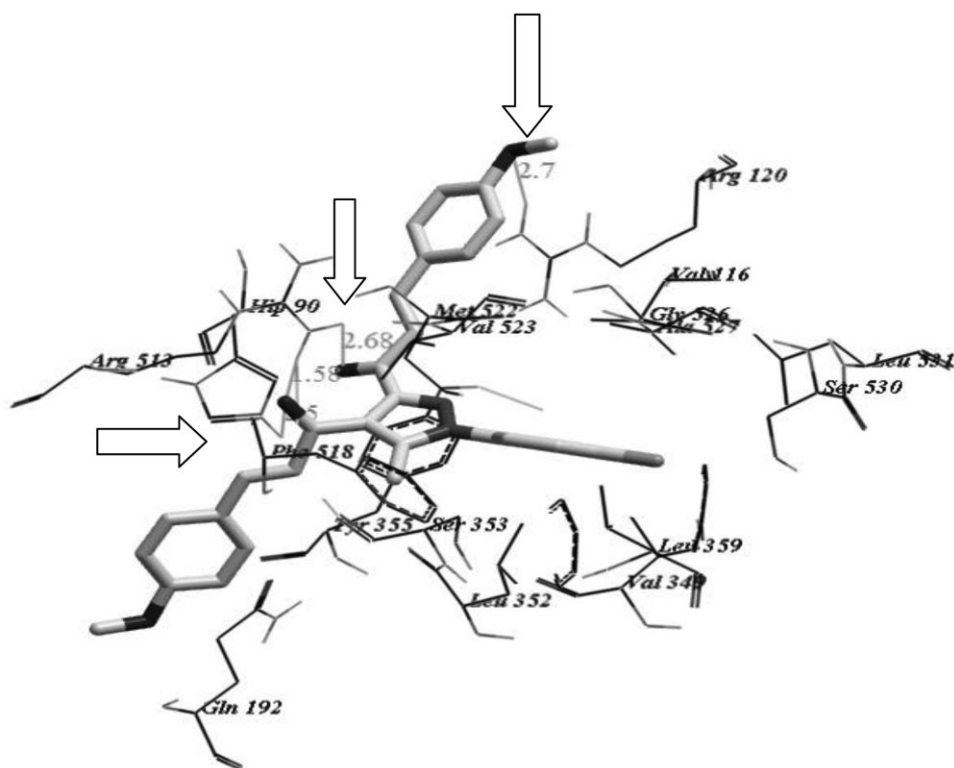


Figure 3. Binding mode of **3c** docked in COX-2 active site (COX-2 PDB file: 1CX2) showing four hydrogen bonds with amino acid residues Arg120, Tyr355, and Hip90 (follow the arrows).

acid essential for activity [22]. Furthermore, *p*-chlorophenyl group was surrounded by a pocket of different amino acids, which are Leu531, Ser530, Leu352, Tyr385, Trp387, and Ala527.

Conclusion

The present study describes the synthesis of some bis-chalcones-*N*-arylpyrazoles **3a-k**, pyrazolo[3,4-*d*]pyridazines

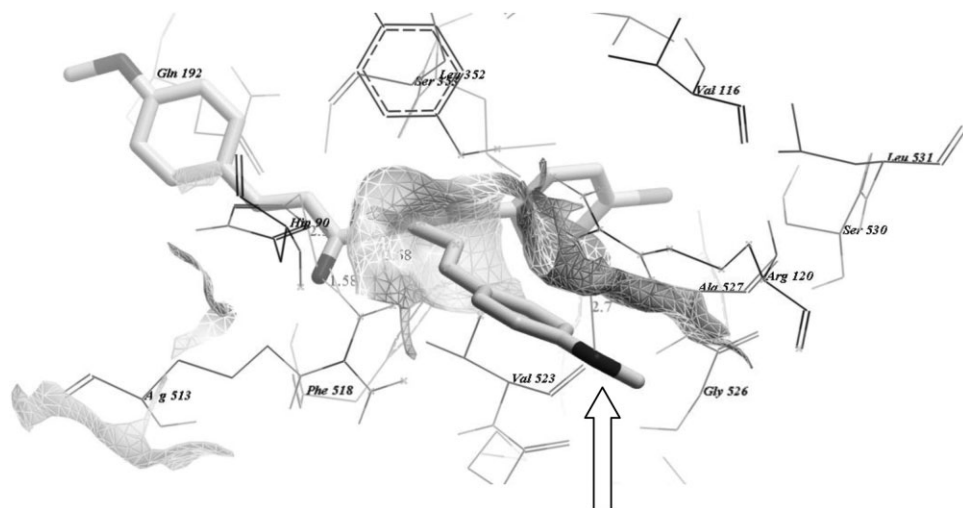


Figure 4. Detailed view about the interaction of the one of the *p*-methoxyphenyl of chalcone wings with important amino acids in the binding site of COX-2 isozyme (follow the arrow).

4a–b, and pyrazolo[3,4-*d*]pyridazine thiocyanate salts **5a–e**. The bis-chalcones *N*-arylpyrazoles revealed anti-inflammatory activity through inhibition of COX-2 enzyme. Compound **3c** showed a suitable inhibitory action for this enzyme with good selectivity index related to the COX-1 enzyme. Further molecular docking studies have been conducted to investigate the binding mode of compound **3c** with the COX-2 isozyme binding site.

Experimental

Chemistry

Melting points (°C, uncorrected) were determined using a Stuart melting point apparatus. The IR spectra (KBr) were recorded on a PerkinElmer FT/IR spectrometer. The NMR spectra were recorded by Varian Gemini-2000 200 MHz FT-NMR spectrometers (Varian, Inc., Palo Alto, CA). Chemical shifts are reported in parts per million (δ), and coupling constants (*J*) are expressed in Hertz. TMS was used as an internal standard, and chemical shifts were measured in δ ppm. ^1H and ^{13}C spectra were run at 200 and 50 MHz, respectively. Electron impact mass spectra were measured on a Varian MAT 311-A (70 eV). Elemental analysis was carried out for C, H, and N at the Microanalytical Center of Cairo University. All reagents were purchased from Sigma-Aldrich Chemical Company.

Synthesis of compounds **2a–e**

A mixture of pentan-2,4-dione (1.34 g, 10 mmol) and the appropriate 2-oxo-*N*-arylpropanehydrazonoyl chloride **1a–e** (10 mmol) in ethanolic sodium ethoxide (10 mol in 20 mL ethanol) was stirred at room temperature for 8 h to afford compounds **2a–e**. Compounds **2a–c** are reported and their experimental data are mentioned in the literature [23, 24].

1,1'-(1-(4-Fluorophenyl)-5-methyl-1H-pyrazole-3,4-diyl)-diethanone (**2d**)

White crystals, 63% yield; mp 155–157°C; IR (KBr) $\nu_{\text{max}}/\text{cm}^{-1}$ 1720, 1725 (2C=O), 1603 (C=N); ^1H NMR (pyridine-*d*₅) δ = 2.38 (s, 3H, $-\text{CH}_3$), 2.69 (s, 3H, $-\text{COCH}_3$), 2.71 (s, 3H, $-\text{COCH}_3$), 7.50–7.78 (dd, 4H, *J* = 7.2 Hz, Ar-H) ppm; ^{13}C NMR (pyridine-*d*₅) δ = 11.70 ($-\text{CH}_3$), 27.61 ($-\text{CH}_3$), 30.13 ($-\text{CH}_3$), 116.43, 116.88, 117.25, 127.52, 135.02, 141.69, 143.79 (aromatic C), 149.01 ($-\text{C}=\text{O}$), 150.43 ($-\text{C}=\text{O}$) ppm. MS *m/z* (%) 260 (M^+ , 100), 246 (M^+ , 97.3), 149 (54.88), 136 (91.7), 95 (68.8). Anal. calcd. for $\text{C}_{14}\text{H}_{13}\text{FN}_2\text{O}_2$ (260.26): C, 64.61; H, 5.03; N, 10.76. Found: C, 64.44; H, 5.02; N, 10.95.

1,1'-(1-(4-Bromophenyl)-5-methyl-1H-pyrazole-3,4-diyl)-diethanone (**2e**)

Pale yellow powder, 57% yield; mp 151–153°C; IR (KBr) $\nu_{\text{max}}/\text{cm}^{-1}$ 1723, 1721 (2C=O), 1587 (C=N); ^1H NMR (pyridine-*d*₅) δ = 2.40 (s, 3H, $-\text{CH}_3$), 2.69 (s, 3H, $-\text{COCH}_3$), 2.71 (s, 3H, $-\text{COCH}_3$), 7.50–7.78 (dd, 4H, *J* = 7.2 Hz, Ar-H) ppm; ^{13}C NMR (pyridine-*d*₅) δ = 12.03 ($-\text{CH}_3$), 27.87 ($-\text{CH}_3$), 31.74 ($-\text{CH}_3$), 123.29, 124.27, 127.93, 133.18, 135.77, 136.26 (aromatic C), 149.64 ($-\text{C}=\text{O}$), 150.72 ($-\text{C}=\text{O}$) ppm. MS *m/z* (%) 323 (M^+ +2, 28.05) 321 (M^+ , 28.25), 165 (23.86), 154 (23.89). Anal. calcd. for $\text{C}_{14}\text{H}_{13}\text{BrN}_2\text{O}_2$ (321.17): C, 52.36; H, 4.08; N, 8.72. Found: C, 52.47; H, 3.70; N, 8.70.

Synthesis of bis-chalcones **3a–k**

To a stirred solution of the appropriate pyrazole **2a–e** (10 mmol) and the appropriate aldehyde (20 mmol) in ethanol (30 mL), 10% aqueous sodium hydroxide (10 mL) was added portionwise at room temperature for 10 min. The reaction mixture was further stirred for 6 h. The resulting solid was filtered, washed with water, dried, and crystallized from EtOH/DMF.

1,1'-(5-Methyl-1-phenyl-1H-pyrazole-3,4-diyl)bis(3-(2,4-dichlorophenyl)prop-2-en-1-one) (**3a**)

Orange crystals, 65% yield; mp >300°C; IR (KBr) $\nu_{\text{max}}/\text{cm}^{-1}$ 1670, 1622 (2C=O), 1570 (C=N); ^1H NMR (pyridine-*d*₅) δ = 2.52 (s, 3H, $-\text{CH}_3$), 7.21–8.52 (m, 17H, Ar-H + olefinic $-\text{CH}=\text{C}$) ppm; ^{13}C NMR (pyridine-*d*₅) δ = 11.77 ($-\text{CH}_3$), 123.00, 123.50, 126.06, 126.42, 127.98, 129.40, 129.68, 129.86, 130.11, 131.27, 134.99, 135.49, 137.98 (aromatic C), 149.28 ($-\text{C}=\text{O}$), 149.81 ($-\text{C}=\text{O}$) ppm; MS *m/z* (%) 558 (M^+ +2, 3.31), (556 (M^+ , 8.9), 521 (1.5), 251 (6.3), 170 (42.74), 135 (100). Anal. calcd. for $\text{C}_{28}\text{H}_{18}\text{Cl}_4\text{N}_2\text{O}_2$ (556.27): C, 60.46; H, 3.26; N, 5.04. Found: C, 60.51; H, 3.29; N, 5.13.

1,1'-(5-Methyl-1-(4-methylphenyl)-1H-pyrazole-3,4-diyl)-bis(3-(2,4-dichlorophenyl)prop-2-en-1-one) (**3b**)

White crystals, 78% yield; mp >300°C; IR (KBr) $\nu_{\text{max}}/\text{cm}^{-1}$ 1695, 1625 (2C=O), 1535 (C=N); ^1H NMR (pyridine-*d*₅) δ = 1.82 (s, 3H, $-\text{CH}_3$), 2.05 (s, 3H, $-\text{CH}_3$), 6.65–7.94 (m, 14H, Ar-H + olefinic $-\text{CH}=\text{C}$) ppm; ^{13}C NMR (pyridine-*d*₅) δ = 12.30 ($-\text{CH}_3$), 21.42 ($-\text{CH}_3$), 123.50, 124.49, 126.41, 128.49, 129.89, 130.86, 131.88, 135.56, 136.49, 138.49 (aromatic C), 149.82 ($-\text{C}=\text{O}$), 150.91 ($-\text{C}=\text{O}$) ppm; MS *m/z* (%) 572 (M^+ +2, 6.31), 570 (M^+ , 14.76), 536 (62.22), 135 (100). Anal. calcd. for $\text{C}_{29}\text{H}_{20}\text{Cl}_4\text{N}_2\text{O}_2$ (570.29): C, 61.08; H, 3.53; N, 4.91. Found: C, 61.12; H, 3.51; N, 4.98.

1,1'-(1-(4-Chlorophenyl)-5-methyl-1H-pyrazole-3,4-diyl)-bis(3-(4-methoxyphenyl)prop-2-en-1-one) (**3c**)

Pale yellow crystals, 59% yield; mp 198–200°C; IR (KBr) $\nu_{\text{max}}/\text{cm}^{-1}$ 1631, 1643 (2C=O), 1598 (C=N); ^1H NMR (pyridine-*d*₅) δ = 2.52 (s, 3H, $-\text{CH}_3$), 3.67 (s, 6H, 2 $-\text{OCH}_3$), 6.94–8.18 (m, 16H, Ar-H and olefinic $-\text{CH}=\text{C}$) ppm; ^{13}C NMR (pyridine-*d*₅) δ = 12.24 ($-\text{CH}_3$), 55.84 (2 $-\text{OCH}_3$), 113.66, 115.21, 121.78, 122.28, 122.78, 126.91, 129.43, 129.72, 133.74, 133.80, 134.22, 134.28, 134.72, 134.79, 141.16, 142.92, 148.69, 149.22 (aromatic C), 162.47 ($-\text{C}=\text{O}$), 162.77 ($-\text{C}=\text{O}$) ppm; MS *m/z* (%) 514 (M^+ +2, 6.71), 512 (M^+ , 14.49), 391 (92.97), 152 (83.31), 132 (100), 89 (88.93), 76 (61.0). Anal. calcd. for $\text{C}_{30}\text{H}_{25}\text{ClN}_2\text{O}_4$ (512.98): C, 70.24; H, 4.91; N, 5.46. Found: C, 70.23; H, 4.97; N, 5.50.

1,1'-(1-(4-Chlorophenyl)-5-methyl-1H-pyrazole-3,4-diyl)-bis(3-(2,4-dichlorophenyl)prop-2-en-1-one) (**3d**)

Pale yellow crystals, 67% yield; mp 247–249°C; IR (KBr) $\nu_{\text{max}}/\text{cm}^{-1}$ 1665, 1654 (2C=O), 1604 (C=N); ^1H NMR (pyridine-*d*₅) δ = 2.54 (s, 3H, $-\text{CH}_3$), 7.20–8.49 (m, 14H, Ar-H + olefinic $-\text{CH}=\text{C}$) ppm; ^{13}C NMR (pyridine-*d*₅) δ = 12.30 ($-\text{CH}_3$), 123.50, 124.50, 126.41, 128.04, 129.95, 130.51, 131.88, 135.47, 136.47, 138.72 (aromatic C), 149.84 ($-\text{C}=\text{O}$), 150.94 ($-\text{C}=\text{O}$) ppm; MS *m/z* (%) 593 (M^+ +2, 2.21), 591 (M^+ , 6.87), 554 (14.69), 518 (9.55), 483 (6.62), 135 (100). Anal. calcd. for $\text{C}_{28}\text{H}_{17}\text{Cl}_5\text{N}_2\text{O}_2$ (590.71): C, 56.93; H, 2.90; N, 4.74. Found: C, 56.63; H, 2.80; N, 4.37.

1,1'-(1-(4-Chlorophenyl)-5-methyl-1H-pyrazole-3,4-diyl)-bis(3-(furan-2-yl)prop-2-en-1-one) (3e)

Pale yellow crystals, 72% yield; mp 194–196 °C; IR (KBr) $\nu_{\max}/\text{cm}^{-1}$ 1669, 1657 (2C=O), 1600 (C=N); ^1H NMR (pyridine- d_5) δ = 2.48 (s, 3H, $-\text{CH}_3$), 6.49–7.99 (m, 14H, Ar-H + olefinic =CH) ppm; ^{13}C NMR (pyridine- d_5) δ = 12.24 ($-\text{CH}_3$), 113.12, 113.27, 116.26, 117.08, 121.03, 123.01, 123.52, 126.06, 127.39, 128.83, 129.87, 130.33, 134.99, 135.08, 135.49, 145.64, 145.93, 149.36 (aromatic C), 149.89 (C=O), 152.03 (C=O) ppm; MS m/z (%) 432 (M^+ , 2.46), 281 (28.18), 207 (100), 73 (52.93). Anal. calcd. for $\text{C}_{24}\text{H}_{17}\text{ClN}_2\text{O}_4$ (432.86): C, 66.59; H, 3.96; N, 6.47. Found: C, 66.37; H, 3.45; N, 6.40.

1,1'-(1-(4-Fluorophenyl)-5-methyl-1H-pyrazole-3,4-diyl)-bis(3-(4-methoxyphenyl)prop-2-en-1-one) (3f)

Creamy white crystals, 70% yield; mp 176–178 °C; IR (KBr) $\nu_{\max}/\text{cm}^{-1}$ 1669, 1657 (2C=O), 1596 (C=N); ^1H NMR (pyridine- d_5) δ = 2.51 (s, 3H, $-\text{CH}_3$), 3.67 (s, 6H, 2-OCH₃), 6.95–8.18 (m, 16H, Ar-H + olefinic $-\text{CH}=\text{C}$) ppm; ^{13}C NMR (pyridine- d_5) δ = 12.24 ($-\text{CH}_3$), 54.07 (2-OCH₃), 113.66, 115.21, 121.78, 122.28, 122.78, 126.91, 129.43, 129.72, 133.74, 133.80, 134.22, 134.28, 134.72, 134.79, 141.16, 142.92, 148.68, 149.22 (aromatic C), 162.47 (C=O), 162.76 (C=O) ppm; MS m/z (%) 497 (M^+ , 8.35), 376 (64.64), 241 (32.9), 161 (51.5), 136 (100). Anal. calcd. for $\text{C}_{30}\text{H}_{25}\text{FN}_2\text{O}_4$ (496.53): C, 72.57; H, 5.07; N, 5.64. Found: C, 72.33; H, 4.90; N, 5.75.

1,1'-(1-(4-Fluorophenyl)-5-methyl-1H-pyrazole-3,4-diyl)-bis(3-(2,4-dichlorophenyl)prop-2-en-1-one) (3g)

Yellow crystals, 55% yield; mp 222–224 °C; IR (KBr) $\nu_{\max}/\text{cm}^{-1}$ 1670, 1678 (2C=O), 1608 (C=N); ^1H NMR (CDCl_3 - d) δ = 2.45 (s, 3H, $-\text{CH}_3$), 7.26–8.26 (m, 14H, Ar-H + olefinic $-\text{CH}=\text{C}$) ppm; ^{13}C NMR (CDCl_3 - d) δ = 13.23 ($-\text{CH}_3$), 117.69, 118.16, 126.91, 128.81, 128.94, 129.08, 129.96, 130.10, 131.24, 131.45, 131.40, 133.07, 137.36, 138.34, 140.16 (aromatic C), 149.34 (C=O), 149.88 (C=O) ppm; MS m/z (%) 576 (M^+ +2, 4.06), 574 (M^+ , 12.26), 539 (100), 136 (40.37). Anal. calcd. for $\text{C}_{28}\text{H}_{17}\text{Cl}_4\text{FN}_2\text{O}_2$ (574.26): C, 58.56; H, 2.98; N, 4.88. Found: C, 58.73; H, 2.60; N, 4.64.

1,1'-(1-(4-Fluorophenyl)-5-methyl-1H-pyrazole-3,4-diyl)-bis(3-(furan-2-yl)prop-2-en-1-one) (3h)

Yellow crystals, 62% yield; mp 166–168 °C; IR (KBr) $\nu_{\max}/\text{cm}^{-1}$ 1669, 1657 (2C=O), 1600 (C=N); ^1H NMR (pyridine- d_5) δ = 2.46 (s, 3H, $-\text{CH}_3$), 6.55–8.1 (m, 14H, Ar-H + olefinic =CH) ppm; ^{13}C NMR (pyridine- d_5) δ = 12.24 ($-\text{CH}_3$), 113.09, 113.23, 116.20, 116.38, 116.85, 117.02, 121.04, 121.04, 122.99, 123.50, 123.99, 126.06, 128.02, 128.20, 128.73, 130.24, 134.96, 135.46, 135.50, 136.00, 145.60, 145.88, 149.34 (aromatic C), 149.87 (C=O), 152.01 (C=O) ppm; MS m/z (%) 417 (M^+ , 17.32), 295 (32.9), 136 (100), 121 (76.01). Anal. calcd. for $\text{C}_{24}\text{H}_{17}\text{FN}_2\text{O}_4$ (416.40): C, 69.23; H, 4.12; N, 6.73. Found: C, 69.01; H, 4.1; N, 6.68.

1,1'-(1-(4-Bromophenyl)-5-methyl-1H-pyrazole-3,4-diyl)-bis(3-(4-methoxyphenyl)prop-2-en-1-one) (3i)

Pale yellow crystals, 67% yield; mp 182–184 °C; IR (KBr) $\nu_{\max}/\text{cm}^{-1}$ 1669, 1657 (2C=O), 1600 (C=N); ^1H NMR (pyridine- d_5) δ = 2.51 (s, 3H, $-\text{CH}_3$), 3.66 (s, 6H, 2-OCH₃), 6.93–8.16 (m, 16H, Ar-H + olefinic =CH) ppm; ^{13}C NMR (pyridine- d_5) δ = 12.24 ($-\text{CH}_3$), 55.85 (2-OCH₃), 115.43, 122.07, 123.52, 124.50, 127.19, 128.22, 128.52, 128.75,

131.16, 131.45, 133.45, 133.49, 136.49, 143.01, 144.78, 149.84, 150.94 (aromatic C), 162.47 (C=O), 162.76 (C=O) ppm; MS m/z (%) 558 (M^+ , 15.88), 438 (50.84), 161 (57.08), 133 (100). Anal. calcd. for $\text{C}_{30}\text{H}_{25}\text{BrN}_2\text{O}_4$ (557.43): C, 64.64; H, 4.52; N, 5.03. Found: C, 64.2; H, 4.44; N, 4.66.

1,1'-(1-(4-Bromophenyl)-5-methyl-1H-pyrazole-3,4-diyl)-bis(3-(2,4-dichlorophenyl)prop-2-en-1-one) (3j)

Pale yellow crystals, 59% yield; mp 244–246 °C; IR (KBr) $\nu_{\max}/\text{cm}^{-1}$ 1678, 1680 (2C=O), 1606 (C=N); ^1H NMR (pyridine- d_5) δ = 2.55 (s, 3H, $-\text{CH}_3$), 7.21–8.52 (m, 14H, Ar-H + olefinic $-\text{CH}=\text{C}$) ppm; ^{13}C NMR (pyridine- d_5) δ = 11.77 ($-\text{CH}_3$), 122.99, 123.50, 127.78, 128.04, 129.46, 130.30, 131.27, 133.30, 135.01, 135.50 (aromatic C), 149.34 (C=O), 149.87 (C=O) ppm; MS m/z (%) 637 (M^+ +2, 10.3), 635 (M^+ , 10.45), 433 (45), 199 (40.37). Anal. calcd. for $\text{C}_{28}\text{H}_{17}\text{BrCl}_4\text{N}_2\text{O}_2$ (635.16): C, 52.95; H, 2.70; N, 4.41. Found: C, 52.66; H, 2.65; N, 4.51.

1,1'-(1-(4-Bromophenyl)-5-methyl-1H-pyrazole-3,4-diyl)-bis(3-(furan-2-yl)prop-2-en-1-one) (3k)

Yellow crystals, 70% yield; mp 195–197 °C; IR (KBr) $\nu_{\max}/\text{cm}^{-1}$ 1689, 1678 (2C=O), 1590 (C=N); ^1H NMR (pyridine- d_5) δ = 2.50 (s, 3H, $-\text{CH}_3$), 6.54–8.17 (m, 14H, Ar-H + olefinic =CH) ppm; ^{13}C NMR (pyridine- d_5) δ = 11.68 ($-\text{CH}_3$), 114.93, 116.44, 116.91, 121.63, 122.99, 123.50, 126.72, 128.16, 128.34, 129.87, 130.66, 130.95, 135.02, 135.50, 142.42, 144.20 (aromatic C), 149.34 (C=O), 152.87 (C=O) ppm; MS m/z (%) 479 (M^+ +2, 3.38), 477 (M^+ , 3.8), 121 (100). Anal. calcd. for $\text{C}_{24}\text{H}_{17}\text{FN}_2\text{O}_4$ (477.31): C, 60.39; H, 3.59; N, 5.87. Found: C, 60.43; H, 3.62; N, 5.91.

Synthesis of compounds 4a–b

To compounds 2d–e (2 mmol) in ethanol (10 mL) hydrazine hydrate (1 mL, 99%) was added and then the reaction mixture was heated at reflux for 8 h. The precipitated product was filtered off, washed with ethanol, dried, and finally crystallized from EtOH/ acetic acid.

2-(4-Fluorophenyl)-3,4,7-trimethyl-2H-pyrazolo[3,4-d]-pyridazine (4a)

Brown crystals, 70% yield; mp 225–227 °C; IR (KBr) $\nu_{\max}/\text{cm}^{-1}$ 1608 (C=N); ^1H NMR (pyridine- d_5) δ = 2.55 (s, 3H, $-\text{CH}_3$), 2.85 (s, 3H, $-\text{CH}_3$), 3.01 (s, 3H, $-\text{CH}_3$), 7.32–7.62 (dd, 4H, J = 7.5 Hz, Ar-H) ppm; ^{13}C NMR (pyridine- d_5) δ = 12.61 ($-\text{CH}_3$), 18.01 ($-\text{CH}_3$), 20.77 ($-\text{CH}_3$), 111.89, 122.99, 123.50, 127.26, 134.97, 135.47, 149.34, 149.89 (aromatic C) ppm; MS m/z (%) 256 (M^+ , 78.14), 238 (100), 168 (15.7), 149 (19.34). Anal. calcd. for $\text{C}_{14}\text{H}_{13}\text{FN}_4$ (256.11): C, 65.61; H, 5.11; N, 21.86. Found: C, 65.45; H, 5.00; N, 21.48.

2-(4-Bromophenyl)-3,4,7-trimethyl-2H-pyrazolo[3,4-d]-pyridazine (4b)

White crystals, 73% yield; mp 268–269 °C; IR (KBr) $\nu_{\max}/\text{cm}^{-1}$ 1606 (C=N); ^1H NMR (pyridine- d_5) δ = 2.57 (s, 3H, $-\text{CH}_3$), 2.85 (s, 3H, $-\text{CH}_3$), 3.00 (s, 3H, $-\text{CH}_3$), 7.21–7.82 (dd, 4H, J = 7.5 Hz, Ar-H) ppm; ^{13}C NMR (pyridine- d_5) δ = 12.50 ($-\text{CH}_3$), 18.27 ($-\text{CH}_3$), 20.77 ($-\text{CH}_3$), 111.89, 122.99, 123.50, 128.33, 132.95, 135.00, 135.50, 149.34, 149.89 (aromatic C) ppm; MS m/z (%) 319 (M^+ +2, 99.59), 317 (M^+ , 100), 237 (24.59), 198 (29.78), 167 (14.24), 154 (43.1). Anal. calcd. for $\text{C}_{14}\text{H}_{13}\text{BrN}_4$ (317.18): C, 53.01; H, 4.13; N, 17.66. Found: C, 53.23; H, 4.32; N, 17.80.

Synthesis of compounds 5a–e

A mixture of compounds 2a–e (1 mmol) and thiosemicarbazide (0.18 g, 2 mmol) in aqueous ethanol (1:1, 50 mL) containing a catalytic amount of acetic acid (0.5 mL) was heated at reflux for 4 h. The precipitated product was filtered off, washed with ethanol, dried, and finally crystallized from EtOH/acetic acid.

3,4,7-Trimethyl-2-phenyl-2H-pyrazolo[3,4-d]pyridazin-5-ium isothiocyanate (5a)

Pink crystals, 65% yield; mp. 238–239°C; IR (KBr) $\nu_{\max}/\text{cm}^{-1}$ 2042 (SCN), 1627 (C=N); ^1H NMR (pyridine- d_5) δ = 2.32 (s, 3H, $-\text{CH}_3$), 2.64 (s, 3H, $-\text{CH}_3$), 2.98 (s, 3H, $-\text{CH}_3$), 7.38–7.67 (dd, 4H, J = 7.45 Hz, Ar-H) ppm; ^{13}C NMR (pyridine- d_5) δ = 12.61 ($-\text{CH}_3$), 18.01 ($-\text{CH}_3$), 20.04 ($-\text{CH}_3$), 123.50, 124.50, 128.54, 130.47, 135.49, 136.49, 149.80, 150.87 (aromatic C) ppm; MS m/z (%) 298 ($\text{M}^+ + 1$, 3.38), 297 (M^+ , 40.8), 252 (100), 168 (18.57). Anal. calcd. for $\text{C}_{15}\text{H}_{15}\text{N}_5\text{S}$ (297.38): C, 60.58; H, 5.08; N, 23.55; S, 10.78. Found: C, 60.77; H, 5.15; N, 23.39; S, 10.66.

3,4,7-Trimethyl-2-(p-tolyl)-2H-pyrazolo[3,4-d]pyridazin-5-ium isothiocyanate (5b)

White crystals, 48% yield; mp. 270–271°C; IR (KBr) $\nu_{\max}/\text{cm}^{-1}$ 2041 (SCN), 1610 (C=N); ^1H NMR (pyridine- d_5) δ = 2.32 (s, 3H, $-\text{CH}_3$), 2.69 (s, 3H, $-\text{CH}_3$), 2.93 (s, 3H, $-\text{CH}_3$), 2.99 (s, 3H, $-\text{CH}_3$), 7.34–7.66 (dd, 4H, J = 7.5 Hz, Ar-H) ppm; ^{13}C NMR (pyridine- d_5) δ = 12.61 ($-\text{CH}_3$), 18.01 ($-\text{CH}_3$), 20.04 ($-\text{CH}_3$), 20.95 ($-\text{CH}_3$), 122.99, 123.50, 126.28, 130.34, 135.02, 135.52, 140.28, 149.31, 149.86 (aromatic C) ppm; MS m/z (%) 311 (M^+ , 25.23), 252 (100), 168 (15.25). Anal. calcd. for $\text{C}_{16}\text{H}_{17}\text{N}_5\text{S}$ (311.40): C, 61.71; H, 5.50; N, 22.49; S, 10.30. Found: C, 61.26; H, 5.20; N, 22.8; S, 10.69.

2-(4-Chlorophenyl)-3,4,7-trimethyl-2H-pyrazolo[3,4-d]pyridazin-5-ium isothiocyanate (5c)

Pale yellow crystals, 62% yield; mp. 267–268°C; IR (KBr) $\nu_{\max}/\text{cm}^{-1}$ 2043 (SCN), 1612 (C=N); ^1H NMR (pyridine- d_5) δ = 2.64 (s, 3H, $-\text{CH}_3$), 2.92 (s, 3H, $-\text{CH}_3$), 2.98 (s, 3H, $-\text{CH}_3$), 7.62–7.79 (dd, 4H, J = 7.5 Hz, Ar-H) ppm; ^{13}C NMR (pyridine- d_5) δ = 12.61 ($-\text{CH}_3$), 18.01 ($-\text{CH}_3$), 20.04 ($-\text{CH}_3$), 123.50, 124.50, 128.54, 130.47, 135.49, 136.49, 149.80, 150.87 (aromatic C) ppm; MS m/z (%) 333 ($\text{M}^+ + 2$, 3.21), 331 (M^+ , 9.67), 272 (100), 168 (12.55). Anal. calcd. for $\text{C}_{15}\text{H}_{14}\text{ClN}_5\text{S}$ (331.82): C, 54.29; H, 4.25; N, 21.11; S, 9.66. Found: C, 54.38; H, 4.2; N, 21.06; S, 9.40.

2-(4-Fluorophenyl)-3,4,7-trimethyl-2H-pyrazolo[3,4-d]pyridazin-5-ium isothiocyanate (5d)

Creamy white crystals, 55% yield; mp. 270–272°C IR (KBr) $\nu_{\max}/\text{cm}^{-1}$ 2044 (SCN), 1608 (C=N); ^1H NMR (pyridine- d_5) δ = 2.64 (s, 3H, $-\text{CH}_3$), 2.93 (s, 3H, $-\text{CH}_3$), 2.98 (s, 3H, $-\text{CH}_3$), 7.36–7.84 (dd, 4H, J = 7.5 Hz, Ar-H) ppm; ^{13}C NMR (pyridine- d_5) δ = 12.56 ($-\text{CH}_3$), 17.90 ($-\text{CH}_3$), 19.89 ($-\text{CH}_3$), 116.57, 117.02, 122.99, 123.50, 126.41, 128.63, 128.81, 133.03, 135.53, 149.25, 149.78 (aromatic C) ppm; MS m/z (%) 315 (M^+ , 3.21), 256 (44.16), 185 (7.6), 136 (29.53). Anal. calcd. for $\text{C}_{15}\text{H}_{14}\text{FN}_5\text{S}$ (315.37): C, 57.13; H, 4.47; N, 21.21; S, 10.17. Found: C, 56.98; H, 4.07; N, 21.31; S, 10.56.

2-(4-Bromophenyl)-3,4,7-trimethyl-2H-pyrazolo[3,4-d]pyridazin-5-ium isothiocyanate (5e)

Pale yellow crystals, 72% yield; mp. 275–276°C; IR (KBr) $\nu_{\max}/\text{cm}^{-1}$ 2046 (SCN), 1608 (C=N); ^1H NMR (pyridine- d_5) δ = 2.659 (s, 3H,

$-\text{CH}_3$), 2.94 (s, 3H, $-\text{CH}_3$), 2.97 (s, 3H, $-\text{CH}_3$), 7.72–7.82 (dd, 4H, J = 7.5 Hz, Ar-H) ppm; ^{13}C NMR (pyridine- d_5) δ = 12.30 ($-\text{CH}_3$), 21.42 ($-\text{CH}_3$), 123.28, 124.27, 128.55, 128.49, 129.97, 132.96, 133.31, 135.27, 136.27, 138.49, 149.61, 150.69 (aromatic C) ppm; MS m/z (%) 378 ($\text{M}^+ + 2$, 2.25), 376 (M^+ , 2.39), 318 (15.31), 257 (4.41), 157 (13.25). Anal. calcd. for $\text{C}_{15}\text{H}_{14}\text{BrN}_5\text{S}$ (376.27): C, 47.88; H, 3.75; N, 18.61; S, 8.52. Found: C, 47.71; H, 3.50; N, 18.47; S, 8.52.

Biological evaluation

Animals

Male albino rats weighing 150–200 g were used. All experimental animals were provided by the Regional Centre of Mycology and Biotechnology, Al Azhar University, Cairo, Egypt. All animals were held under standard laboratory conditions in the animal house (temperature 25°C) with a 12/12 light–dark cycle. Animals were fed laboratory diet and water *ad libitum*. All experiments were carried out using six animals per group. The animal experiments were performed in accordance with international guidelines.

Drugs

Carrageenan (carrageenan kappa-type III) and all other reagents were purchased from Sigma Chemical Co. (St. Louis, MO, USA).

In vivo anti-inflammatory activity

The test compounds were evaluated using the *in vivo* rat carrageenan-induced foot paw edema model reported previously [19]. The dose for the reference drugs and the test compounds was 10 mmol/kg, given orally.

Test compounds and celecoxib were suspended in gum acacia (7%). The diameter of the right paw of each animal was determined using a micrometer. The control group received only the corresponding vehicle. Thirty minutes later, paw edema was induced by subcutaneous injection of 0.1 mL of carrageenan (0.1%) into the subplantar surface of the right hind paw of all animals. The paw diameter was measured 3 and 6 h after carrageenan injection and is recorded in Table 1.

Ulcerogenic activity

The compounds 3c, 3e, 3f, and 3i, which exhibited the highest anti-inflammatory activity, were investigated for their ulcerogenic activity [20]. Male albino rats weighing 150–200 g were fasted for 12 h prior to drug administration. Water was supplied *ad libitum*. The animals were divided into seven equal groups (each of six). The first group received 7% gum acacia (suspending vehicle) orally once a day and was left as a control, whereas the other groups received the reference drugs and test compounds with a dose of 100 mmol/kg/day orally. The test compounds were administered once a day for three successive days. The animals were killed by an overdose of ether 6 h after the last dose. The stomachs were removed, opened along the greater curvature, and examined for ulceration. The number and diameter of discrete areas of damage in the glandular mucosa were scored (Table 1). The ulcer score was calculated according to the method of Vijaya and Mishra [20]: 0.0 – normal (no injury); 0.5 – latent injury; 1.0 – slight injury (two to three dotted lines); 2.0 – severe injury (continuous lined injury or five to six dotted injuries); 3.0 – very severe injury (several continuous lined injuries); 4.0 – widespread lined injury.

Statistics

In anti-inflammatory study, data were expressed as value \pm SEM. Results of carrageenan-induced paw edema experiments were also expressed as percentage of change from control (pre-drug) values. Differences between vehicle control and treatment groups were tested using one-way ANOVA followed by multiple comparisons using Bonferroni's test. In ulcerogenic study, data were presented as mean \pm SE and were subjected to one-way ANOVA, followed by multiple comparisons using Bonferroni's test.

In vitro cyclooxygenase inhibition studies

The selected compounds were tested for their ability to inhibit COX-1 and COX-2 using a COX(ovine) inhibitor screening kit (Catalog No. 560101, Cayman Chemical, Ann Arbor, MI) according to the manufacturer's instructions. Cyclooxygenase catalyzes the first step in the biosynthesis of arachidonic acid (AA) to PGH₂. PGF_{2 α} , produced from PGH by reduction with stannous chloride, is measured by EIA (ACE competitive EIA). Stock solutions of test compounds were dissolved in a minimum volume of DMSO. Briefly, to a series of supplied reaction buffer solutions (960 μ L, 0.1 M Tris-HCl pH 8.0 containing 5 mM EDTA and 2 mM phenol) with either COX-1 or COX-2 (10 μ L) enzyme in the presence of heme (10 μ L) was added 10 μ L of various concentrations of test drug solutions (0.001, 0.01, 0.1, 1, 10, 100, and 500 μ M in a final volume of 1 mL). These solutions were incubated for a period of 2 min at 37°C, after which 10 μ L of arachidonic acid (100 μ M) was added, and the COX reaction was stopped by the addition of 50 μ L of 1 M HCl after 2 min. PGF_{2 α} , produced from PGH by reduction with stannous chloride, was measured by EIA. This assay is based on the competition between PGs and a PG-acetylcholinesterase conjugate (PG tracer) for a limited amount of PG antiserum. The amount of PG tracer that is able to bind to the PG antiserum is inversely proportional to the concentration of PGs in the wells since the concentration of the PG tracer is held constant while the concentration of PGs varies. This antibody PG complex binds to a mouse anti-rabbit monoclonal antibody that had been previously attached to the well. The plate is washed to remove any unbound reagents and then Ellman's reagent, which contains the substrate to acetylcholinesterase, is added to the well. The product of this enzymatic reaction produces a distinct yellow color that absorbs at 405 nm. The intensity of this color, determined spectrophotometrically, is proportional to the amount of PG tracer bound to the well, which is inversely proportional to the amount of PGs present in the well during incubation: absorbance [bound PG tracer] / PGs. Percent inhibition was calculated by comparison of compound treated to various control incubations. The concentration of the test compound causing 50% inhibition (IC₅₀, μ M) was calculated from the concentration inhibition response curve (duplicate determinations).

Molecular docking methodology

Docking experiments were performed using ICM-Pro software (version 3.3-02a) by Molsoft. The coordinates for the X-ray crystal structure of the enzymes COX-2 were obtained from the RCSB Protein Data Base (COX-2 PDB file: 1CX2) [8]. The structure data were revised by adding the missing aromatic π systems and ionic attributes to the amino acids in the binding pocket and by adding hydrogen to all amino acids. The revised protein data were converted into the ICM format; the binding pockets were defined by searching the neighbors of the co-crystallized structure of COX-

2 and SC-558; the receptor grid maps were calculated with a grid spacing of 0.5 Å; the grid was defined in such a way that it included the ligand and key residues in each of the x, y, and z directions [25]. For the ligands, 2D–3D conversion is followed by energy minimization using the MMFF option as a force field. The docking algorithm implemented in ICM-Pro (version 3.3-02a) optimized the entire ligand in the receptor field, applying a multistart Monte Carlo minimization procedure in internal coordinate space.

In order to study the interactions, we used the docking software ICM-Pro (version 3.3-02a) and the COX-2 enzyme protein data co-crystallized with SC-558 (PDB entry: 1CX2). After converting the PDB data into an ICM format, defining the receptor active site, and generating the receptor grid maps, we were able to calculate the interaction of our compounds with COX-2.

The authors extend their appreciation to The Regional Centre for Mycology and Biotechnology, Al Azhar University, Cairo, Egypt for providing the facilities to perform the biological evaluation.

The authors have declared no conflict of interest.

References

- [1] I. Tabas, C. K. Glass, *Science* **2013**, 339, 166–172.
- [2] M. M. Hassan, S. A. Khan, A. H. Shaikat, M. E. Hossain, M. A. Hoque, M. H. Ullah, S. Islam, *Vet. World* **2013**, 6, 68–71.
- [3] M. J. Langman, D. M. Jensen, D. J. Watson, S. E. Harper, P.-L. Zhao, H. Quan, J. A. Bolognese, T. J. Simon, *JAMA* **1999**, 282, 1929–1933.
- [4] D. J. Cochrane, B. Jarvis, G. M. Keating, *Drugs* **2002**, 62, 2637–2651.
- [5] A. Di Fiore, C. Pedone, K. D'Ambrosio, A. Scozzafava, G. De Simone, C. T. Supuran, *Bioorg. Med. Chem. Lett.* **2006**, 16, 437–442.
- [6] S. Dadiboyena, A. T. Hamme Ii, *Curr. Org. Chem.* **2012**, 16, 1390–1407.
- [7] R. J. Bing, M. Lomnicka, *J. Am. Coll. Cardiol.* **2002**, 39, 521–522.
- [8] R. G. Kurumbail, A. M. Stevens, J. K. Gierse, J. J. McDonald, R. A. Stegeman, J. Y. Pak, D. Gildehaus, J. M. iyashiro, T. D. Penning, K. Seibert, P. C. Isakson, W. C. Stallings, *Nature* **1996**, 384, 644–648.
- [9] Y. K. Rao, S.-H. Fang, Y.-M. Tzeng, *Biorg. Med. Chem.* **2009**, 17, 7909–7914.
- [10] F. Herencia, M. L. Ferrándiz, A. Ubeda, I. Guillén, J. N. Dominguez, J. E. Charris, G. M. Lobo, M. J. Alcaraz, *Free Radic. Biol. Med.* **2001**, 30, 43–50.
- [11] O. I. El-Sabbagh, S. M. Ibrahim, M. M. Baraka, H. Kothayer, *Arch. Pharm.* **2010**, 343, 274–281.
- [12] A. Araico, M. C. Terencio, M. J. Alcaraz, J. N. Domínguez, C. León, M. L. Ferrándiz, *Life Sci.* **2006**, 78, 2911–2918.
- [13] M. Ismail, J. Lehmann, D. Abou El Ella, A. Albohy, K. Abouzid, *Med. Chem. Res.* **2009**, 18, 725–744.
- [14] H. A. Abdel-Aziz, K. A. Al-Rashood, K. E. H. ElTahir, H. S. Ibrahim, *J. Chin. Chem. Soc.* **2011**, 58, 863–868.

- [15] A. Araico, M. C. Terencio, M. J. Alcaraz, J. N. Domínguez, C. León, M. L. Ferrándiz, *Life Sci.* **2007**, *80*, 2108–2117.
- [16] G. S. B. Viana, M. A. M. Bandeira, F. J. A. Matos, *Phytomedicine* **2003**, *10*, 189–195.
- [17] E. Nassar, H. A. Abdel-Aziz, H. S. Ibrahim, A. M. Mansour, *Sci. Pharm.* **2011**, *79*, 507–524.
- [18] H. A. Abdel-Aziz, A. Bari, S. W. Ng, *Acta Crystallogr. Sect. E* **2010**, *66*, o3344.
- [19] C. A. Winter, E. A. Risley, G. W. Nuss, *Proc. Soc. Exp. Biol. Med.* **1962**, *111*, 544–547.
- [20] K. S. G. Vijaya, D. N. Mishra, *Methods Find. Exp. Clin. Pharmacol.* **2006**, *28*, 419–422.
- [21] K. M. Amin, M. M. Kamel, M. M. Anwar, M. Khedr, Y. M. Syam, *Eur. J. Med. Chem.* **2010**, *45*, 2117–2131.
- [22] O. Llorens, J. J. Perez, A. Palomer, D. Mauleon, *J. Mol. Graph. Modell.* **2002**, *20*, 359–371.
- [23] R. S. Tewari, P. Parihar, *Indian J. Chem. Sect. B* **1980**, *19*, 217–218.
- [24] A. A. Fahmi, *Int. J. Chem.* **1995**, *6*, 1–4.
- [25] V. Maiorov, R. Abagyan, *Fold. Des.* **1998**, *3*, 259–269.